Band-structural and Fourier-spectral properties of one-dimensional generalized Fibonacci lattices

G. Y. Oh and M. H. Lee
Department of Physics, Seoul National University, Seoul 151-742, Korea
(Received 3 June 1993)

We study the electronic and Fourier-spectral properties of one-dimensional generalized Fibonacci lattices generated by the stacking rule $S_{l+1}=S_l^n S_{l-1}^m$ with positive integers n and m, where S_l is the lth generational binary sequence. After showing that, in the limit of the large potential strength, the energy spectrum of a lattice with certain specific n and m can be determined by the associated characteristic value $\tau(n,m)$, we investigate the relation between the electronic band structure and the Fourier spectrum. When the lattice possesses the Pisot-Vijayaraghavan (PV) property (i.e., when $n+1>m$), the Fourier spectrum is closely related to the electronic band structure; the location and the relative strength of the Fourier spectral peak is in agreement with the location and the relative width of the energy spectral gap. On the other hand, when the lattice possesses no PV property (i.e., when $n+1\leq m$), the Fourier spectrum is not directly related to the electronic band structure; the strength of the Fourier spectral peak is irrelevant to the width of the energy spectral gap, while the location of the peak corresponds to that of the gap. We also study the dependence of the electronic and Fourier-spectral properties on the initial conditions of the stacking rule through detailed study of the copper mean lattice $(n=1,m=2)$ with initial conditions $S_1=\{A\}$ and $S_2=\{AB^p\}$. It is found that the fractal structure of the energy spectrum is independent of the integer p, while some local electronic properties depend on p. It is also found that the global structure of the Fourier spectrum depends on p; it looks more blurred, and thus the aperiodic nature of the lattice becomes clearer with the increase of p.

I. INTRODUCTION

During the past decade, much interest has been attracted to the study of substitutional structures,[1–38] which was inspired by the discovery of quasicrystals[7] and the development of layer-growth techniques such as molecular-beam epitaxy.[8] The majority of works have focused on quasiperiodic lattices, and a number of interesting properties have been established. Among other things, it is well established that the energy spectrum of the Fibonacci lattice, a one-dimensional version of quasicrystals, forms a Cantor set with zero Lebesgue measure[2] and that the corresponding electronic states are critical ones showing either self-similar or chaotic wave functions. Despite the absence of periodicity in the sequence, the Fibonacci lattice shows a long-range order such that the Fourier spectrum of the lattice contains Bragg peaks.

Together with quasiperiodic lattices, other kinds of substitutional lattices[9–38] have been extensively studied. The well-known example is the Thue-Morse lattice[10–15] whose sequence is generated by the binary substitution rule $\{A\rightarrow AB, B\rightarrow BA\}$ starting with the letter A. The Thue-Morse lattice exhibits intricate Fourier-spectral and electronic properties. The Fourier-spectral measure of the lattice is known to be a singular continuous one (i.e., neither a discrete one nor an absolutely continuous function of the spectrum),[11–13] which indicates that the order of periodicity can be considered to be in between the orders of quasiperiodic and disordered lattices; quasiperiodic lattices have a discrete atomic measure with Bragg peaks, while disordered lattices have an absolutely continuous one. Contrary to the results of the Fourier spectrum, studies of the electronic properties suggest that the Thue-Morse lattice is in between the electronic properties of the periodic and quasiperiodic lattices.[10,14] To put it concretely, the electronic states of the Thue-Morse lattice consist of extended and critical states; the former is a feature of the periodic lattice, while the latter is a characteristic of the quasiperiodic lattice. Besides, there is no state exponentially localized, which is a distinctive feature from the disordered lattice. Therefore, considering the question of where the Thue-Morse lattice can be located, there seems to be an inconsistency between the results of the electronic and Fourier spectra of the lattice.

The inconsistency mentioned above is not peculiar to the Thue-Morse lattice, but occurs in other kinds of substitutional lattices such as the generalized Fibonacci (GF) lattices.[20–35] The GF sequences are defined by the binary substitutional rule

$$A\rightarrow A^n B^m\ ,\quad B\rightarrow A\ , \tag{1}$$

where n and m are positive integers and A^n represents a string of n A's. Another definition can be provided by the stacking rule

$$S_{l+1}=S_l^n S_{l-1}^m\ , \tag{2}$$

where S_l is the lth generational sequence. After the works of Gumbs and Ali,[20] a number of studies have been devoted to the electronic properties of the GF lattices. When classifying the lattice into two classes according to the criterion of Gumbs and Ali, a lattice belonging to the $(n>1,\ m=1)$ class is known to have a volume-preserving trace map[20,23,24] and a Cantor-like energy spectrum with critical electronic states, while a lattice in the $(n=1,\ m>1)$ class is known to have a volume-

0163-1829/93/48(17)/12465(13)/$06.00

nonpreserving trace map and Bloch-like part as well as the singular part of the energy spectrum such that extended electronic states are allowed.[22,25,26] Fourier spectra of the lattices are also known to have different properties depending on where the lattices belong. The Fourier spectrum of a lattice belonging to the ($n>1$, $m=1$) class contains Bragg peaks; it is called *quasiperiodic* like the ordinary Fibonacci lattice ($n=m=1$). Meanwhile, the Fourier spectrum of a lattice belonging to the ($n=1$, $m>1$) class shows different behavior from that of the ordinary Fibonacci lattice, and the lattice is called *aperiodic*. An aperiodic lattice, a nonperiodic lattice with long-range order whose Fourier transform has no Bragg peak, is generally considered to lie in between quasiperiodic and disordered lattices.[33] Thus, in a lattice belonging to the ($n=1$, $m>1$) class, a similar situation to that of the Thue-Morse lattice occurs.

However, there seems to be no methodology with which to reconcile the seeming inconsistency between the results of electronic and Fourier spectra, which is one of the motives of our study. In Sec. II we perform a systematic study of the electronic band structures of the GF lattices by means of the idea of an approximated renormalization-group (RG) technique which is valid in the limit of large potential strength. We show that the integrated density of states (IDOS) can be determined by a characteristic value $\tau(n,m)$, which can be thought as a generalization of the gap labeling rule for the ordinary Fibonacci lattice.[5] In Sec. III we study the Fourier-spectral properties of the GF lattices. After showing that the structure of the Fourier spectrum strongly depends on the arithmetic property of the GF number, we investigate the connection between the IDOS and the Fourier-spectral peaks, which makes it easier to understand why the results of the Fourier spectra for some lattices differ from those of the electronic properties.

Another motive of the study lies in the initial conditions of Eq. (2). The conventional choice of the initial conditions is to set $S_0=\{B\}$ and $S_1=\{A\}$ such that one has $S_2=\{A^nB^m\}$. In fact, in Secs. II and III this choice is adopted. However, one can easily check that the statistics of elements A and B strongly depends on the initial conditions. Thus the question of what happens if one chooses different initial conditions arises immediately. In Sec. IV we examine the effects of different initial conditions on the electronic and Fourier-spectral properties through a detailed study of a specific example of the GF lattices, the so-called copper mean ($n=1$, $m=2$) lattice. A brief summary is presented in Sec. V.

II. ELECTRONIC BAND STRUCTURE

In the following we consider a tight-binding model defined by

$$t_{n+1,n}\psi_{n+1}+t_{n-1,n}\psi_{n-1}+V_n\psi_n=E\psi_n \ , \tag{3}$$

where the hopping parameter $t_{n\pm1,n}$ ($\equiv T$) is set to be constant and the site energy V_n takes on two values V_A and V_B arranged in the GF sequences.

In case of the ordinary Fibonacci lattice, Niu and Nori[3] introduced an approximated RG scheme to a transfer (or off-diagonal) tight-binding model and explained the trifurcating behavior of the energy spectrum. Liu and Sritrakool[4] adopted the same scheme to the on-site (or diagonal) tight-binding model and illustrated the four-subband global structure as well as the trifurcating behavior of sub-subbands in the following hierarchies. The idea of the scheme is as follows. In the limit of the large potential strength [i.e., $|T/(V_A-V_B)|\ll1$], there exist three kinds of constructing elements $\{B, A, AA\}$ whose energies are denoted by $\{E_B, E_A, E_{A^2}^{(\pm)}\}$, and these construct four subbands (B, AA^-, A, and AA^+ subbands in ascending order of the energy), resulting in a four-subband global structure. Since the dominant effect in the lowest order of approximation is the resonant coupling of the states with the same energy, each of the four subbands can be treated independently of the others. The decomposition produces four chains, all of which can be regarded as transfer models with modified strengths of the hopping parameters. Thus the trifurcating behavior of the sub-subbands can be explained following the lines of the Niu-Nori argument. Since the approximated RG scheme gives a simple and clear picture of the Fibonacci lattice, we adopt the scheme and try to determine the band structures systematically.

A. Generalized Fibonacci numbers

The GF number F_l in the lth generational sequence is given by the recursion relation

$$F_{l+1}=nF_l+mF_{l-1} \ , \tag{4}$$

with initial values $\{F_1=1, F_2=n+m\}$. The characteristic value $\tau(n,m)$, namely, the ratio of F_l to F_{l-1} in the limit of $l\to\infty$, is given by the positive solution of the quadratic equation

$$\tau^2-n\tau-m=0 \tag{5}$$

or explicitly by $\tau(n,m)=[n+\sqrt{n^2+4m}\,]/2$. Here the values of $\tau(n,m)$ for $(n,m)=(1,1)$, $(2,1)$, $(3,1)$, $(1,2)$, $(1,3)$, and $(2,2)$ are conventionally called golden mean, silver mean, bronze mean, copper mean, nickel mean, and mixed mean, respectively. The GF number can also be written as

$$F_l=\frac{1}{\tau_+-\tau_-}[(1-\tau_-)\tau_+^l+(\tau_+-1)\tau_-^l] \ , \tag{6}$$

where τ_+ (τ_-) is the positive (negative) solution of Eq. (5) and τ_+^l (τ_-^l) is the lth power of τ_+ (τ_-). Note that Eqs. (5) and (6) are very important in the study of the Fourier-spectral properties; the arithmetic property of $\tau_\pm$, and thus F_l, turns out to be a crucial factor in determining whether or not the Fourier spectra have anything to do with the energy spectral structures of the GF lattices.

In the case of the ordinary Fibonacci lattice, it suffices to consider the Fibonacci number F_l with $n=m=1$ alone, which implies that the electronic band structure of the lattice is totally characterized by the number defined in Eq. (4). However, in the GF lattices, additional numbers should be considered in order to describe the physi-

cal properties appropriately. Let us denote them as G_l and H_l, which are defined by the same recursion relation as that of F_l but with different initial values, i.e., $\{G_1=1, G_2=n\}$ and $\{H_1=1, H_2=n-1\}$, respectively. Because of the same recursion relation, the three kinds of numbers have the same characteristic value $\tau(n,m)$ and the relations between them are given by

$$F_l=G_l+mG_{l-1}\ , \tag{7a}$$

$$G_l=H_l+G_{l-1}\ . \tag{7b}$$

Note that, when $n=1$, the numbers G_l and H_l can be written as $G_l=F_{l-1}$ and $H_l=mF_{l-3}$ and the corresponding lattices can be characterized by the number F_l alone, as in the ordinary Fibonacci lattice.

B. IDOS and gap labeling rule

A lattice with certain specific n and m consists of three kinds of constructing elements denoted by $\{B^m, A^n, A^{n+m}\}$. The numbers of constructing elements and the total number of the elements in the lth generational sequence are given by

$$N^l_{B^m}=G_{l-1}\ ,\quad N^l_{A^n}=H_{l-1}\ ,\quad N^l_{A^{n+m}}=G_{l-2}\ , \tag{8a}$$

$$N_l(=F_l)=mN^l_{B^m}+nN^l_{A^n}+(n+m)N^l_{A^{n+m}}\ . \tag{8b}$$

The number of global subbands is easily obtained; it is $2(n+1)$ for a lattice with $(n\geq 1, m=1)$, while $2m+1$ or $2(m+1)$ for a lattice with $(n=1, m\geq 1)$ depending on whether m is even or odd.

Each of the global subbands contains one of $\{G_{l-1},H_{l-1},G_{l-2}\}$ eigenvalues such that the density of states on any subband, in the limit of $l\rightarrow\infty$, takes one of the values

$$\{1/(\tau+m),(\tau-1)/[\tau(\tau+m)],1/[\tau(\tau+m)]\}\ ,$$

where $\tau=\tau_+$. Besides, since each sub-subband at any hierarchy has one of $\{G_{l-r},H_{l-r},G_{l-r-1}\}$ eigenvalues, the density of states on any sub-subband takes one of the values

$$\{1/[\tau^{r-1}(\tau-m)],(\tau-1)/[\tau^r(\tau+m)],1/\tau^r[(\tau+m)]\}\ .$$

From these, it is expected that the IDOS at energy E, $N(E)$, is of the form $(a'\tau+b')/[\tau^{r'}(\tau+m)]$ with integers a', b', and r'. Thus, by using the equalities

$$\frac{1}{\tau+m}=\frac{n+m-\tau}{m(n+m-1)}\ , \tag{9a}$$

$$\frac{1}{\tau^r}=\frac{(-1)^r}{m^r}(G_{r+1}-G_r\tau)\ , \tag{9b}$$

the IDOS can be written as

$$N(E)=\frac{a\tau+b}{m^r(n+m-1)}\ , \tag{10}$$

where a, b, and r are integers satisfying $0<N(E)<1$. Equation (10) is the generalization of the gap labeling rule found in the ordinary Fibonacci lattice.[5] By using Eq. (10), locations of the gaps at any hierarchy of a lattice with certain specific n and m can be uniquely characterized. In case of the ordinary Fibonacci lattice, it is well known that the integer a in Eq. (10) increases progressively when one goes to a higher hierarchy and that the largest gap corresponds to the smallest integer. We do not succeed in elucidating the relation between the integer and width of gaps explicitly, but one can conjecture from Eq. (9b) that the integer corresponding to the gap which appears in a higher hierarchy may become larger. It is worth noting that the location of the largest gap N_{mg} is characterized by $(a,b;r)=(-1,n+m;0)$, i.e.,

$$N_{mg}=\frac{m}{\tau+m}=\frac{-\tau+n+m}{n+m-1}\ , \tag{11}$$

which is just the fraction of the number of the element B to the total number of elements. In connection with this, see Ref. 32, where the vibrational properties of the GF lattices are studied and an expression similar to Eq. (11) is given for the integrated density of vibrational states.

Figures 1–3 show the numerically calculated IDOS for three typical examples of the GF lattices, the silver mean $(n=2, m=1)$, the copper mean $(n=1, m=2)$, and the nickel mean $(n=1, m=3)$ lattices, respectively. Even though the calculations are performed both for small lattice sizes ($l=9$, 11, and 9, respectively) and for potential strengths not strong enough ($T/|V_A-V_B|=\frac{1}{3}$, $\frac{1}{4}$, and $\frac{1}{4}$, respectively), the data are in agreement with Eq. (10). Denoting the IDOS as $N(E)=(a\tau+b)/2$ in the silver mean lattice, the values of (a,b) for the five main gaps are labeled by $(-1,3)$, $(2,-4)$, $(-2,6)$, $(1,-1)$, and $(-3,9)$, respectively. In the copper mean lattice, $\tau=2$ enables one to write the IDOS as $N(E)=k/2^r$ with integers k and r, and the values of (k,r) for the four main gaps are given by (1,2), (1,1), (5,3), and (7,3), respectively. In the nickel mean lattice, the IDOS is given by $N(E)=(a\tau+b)/3^r$, and the values of $(a,b;r)$ for the seven main gaps are given by $(-1,4;2)$, $(-2,8;2)$, $(-1,4;1)$, $(-5,29;3)$, $(-1,22;3)$, $(26,123;4)$, and $(-4,34;3)$, respectively.

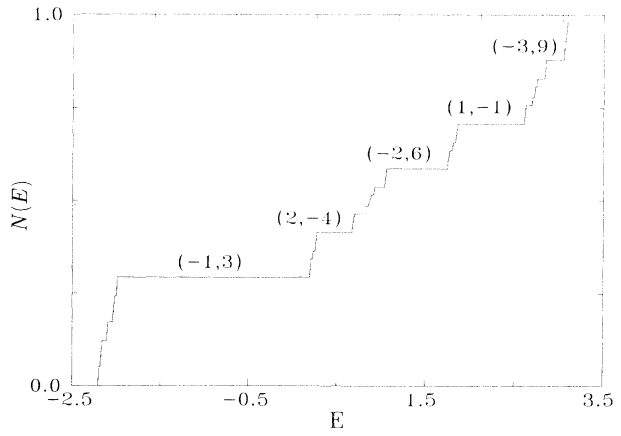

FIG. 1. IDOS vs E for the silver mean lattice. The system size is $N=1393$ $(l=9)$. We take $V=V_A=-V_B=1.5$ and $T=1$. The IDOS is characterized by (a,b) where $N(E)=(a\tau+b)/2$.

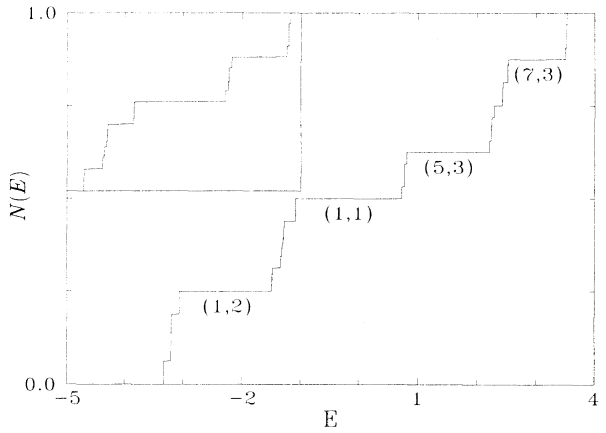

FIG. 2. IDOS vs E for the copper mean lattice. The system size is $N=1365$ ($l=11$). We take $V=V_A=-V_B=2$ and $T=1$. The IDOS is characterized by (k,r) where $N(E)=k/2^r$. The inset represents the fourth main subband which is a mixed subband of monatomic (A) and triatomic (A^3) elements. Compare it with the inset of Fig. 8.

III. FOURIER-SPECTRAL PROPERTIES

A basic step to investigate a substitutional lattice is to study the Fourier spectrum of the lattice. After the pioneering work of Bombieri and Taylor,[6] characteristic values associated with a given substitution rule are known to play a crucial role in determining the properties of the Fourier spectrum. Bombieri and Taylor studied the connections between quasiperiodic lattices and algebraic number theory and showed that a given lattice contains Bragg peaks whenever the characteristic values possess the Pisot-Vijayaraghavan (PV) property that only one of the characteristic values in absolute is larger than unity. As for the GF lattices, the characteristic values are given by the solutions ($\tau_\pm$) of Eq. (5), and it can be easily checked that the characteristic values possess the PV property only if $n+1>m$, while do not possess the property when $n+1<m$, Meanwhile, the condition of $n+1=m$ is a marginal case of the PV property. Even though the definition of the Fourier transform that we take [see Eq. (13)] is different from that of Bombieri and Taylor, the property of the Fourier spectrum is strongly dependent on whether or not the characteristic values possess the PV property, and it can be expected that a lattice is quasiperiodic when $n+1>m$ and aperiodic when $n+1\leq m$.

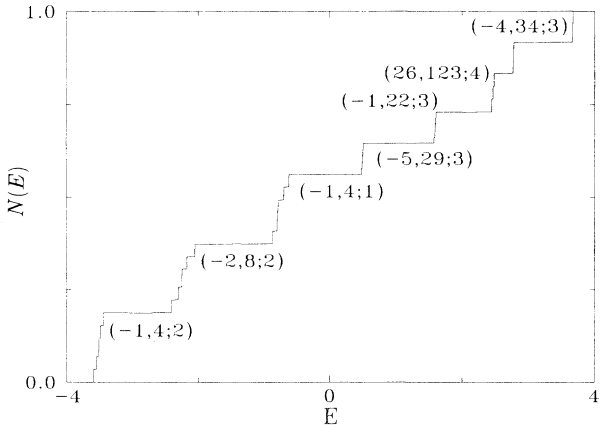

FIG. 3. IDOS vs E for the nickel mean lattice. The system size is $N=1159$ ($l=9$). We take $V=V_A=-V_B=2$ and $T=1$. The IDOS is characterized by $(a,b;r)$ where $N(E)=(a\tau+b)/3^r$.

In periodic or quasiperiodic lattices, Fourier-spectral peaks are closely related to the energy spectral gaps. To be precise, the location and strength of Bragg peaks correspond to the location and width of energy spectral gaps. Is this generically valid for any kind of the GF lattices? Our results given below suggest that, when $n+1>m$, this is valid. On the other hand, when $n+1\leq m$, the relative widths of the energy spectral gaps have nothing to do with the strength of the Fourier-spectral peaks, although the locations of the gaps are related to those of the peaks. The reason for this lies in the fact that the electronic band structures of the GF lattices are insensitive to whether or not the associated characteristic values possess the PV property, while the nature of the Fourier spectra strongly depends on the PV property of the characteristic values. Let us consider the global structural property of the Fourier spectrum and study the relation of the Fourier spectra and the electronic band structures of the GF lattices.

A. Fourier transform

When two types of diffraction centers associated with the GF sequences exist, the scattering property of the lattice is described by a function

$$g(x)=\sum_{k=1}^{F_l}\varepsilon_k\delta(x-k)\ , \tag{12}$$

where ε_k takes on two possible values ε_A and ε_B. Distances between neighboring centers are set to be unity. The Fourier transform of the function can be defined by[12]

$$G_l(\omega)=\sum_{k=1}^{F_l}\varepsilon_k e^{2\pi i\omega k}\ , \tag{13}$$

and the partial structure factor, or Fourier intensity, $S_l(\omega)$ is given by

$$S_l(\omega)=\frac{1}{F_l}|G_l(\omega)|^2\ . \tag{14}$$

When the Fourier amplitude $G_l(\omega)$ is assumed to scale as $|G_l(\omega)|\sim F_l^{\gamma(\omega)}$, the scaling exponent $\gamma(\omega)$ shows different behaviors depending on the nature of the spectral peak,[13] $\gamma(\omega)=1$ for Bragg peaks and $\gamma(\omega)\simeq 1/2$ for a diffuse scattering appearing in disordered structures. Meanwhile, $\gamma(\omega)$ can take diverse values for a singular scattering appearing in, for example, the Thue-Morse lattice and the behavior of $G_l(\omega)$ becomes complicated.

An efficient way for evaluating Eq. (13) is provided by the recursion relation of the Fourier amplitudes. Using

the self-similarity of the GF lattices, one can easily deduce the recursion relation as

$$\begin{bmatrix} G_{l+1}(\omega) \\ G_l(\omega) \end{bmatrix} = \underline{M}_l(\omega) \begin{bmatrix} G_l(\omega) \\ G_{l-1}(\omega) \end{bmatrix} , \tag{15}$$

where $\underline{M}_l(\omega)$ is a 2×2 matrix given by

$$\underline{M}_l(\omega) = \begin{bmatrix} \sum_{j=0}^{n-1} e^{2\pi i j \omega F_l} & \sum_{j=0}^{m-1} e^{2\pi i \omega (nF_l + jF_{l-1})} \\ 1 & 0 \end{bmatrix} . \tag{16}$$

Much information on the behavior of $G_l(\omega)$ can be extracted from the behavior of the arguments of $\underline{M}_l(\omega)$, since the l dependence of $\underline{M}_l(\omega)$ is carried by its arguments. Defining $\omega_l \equiv \omega F_l$ and $\omega_l^{(j)} \equiv n\omega_l + j\omega_{l-1}$, it can be easily checked that there exist Bragg peaks if the two conditions

$$\omega_l \bmod 1 \to 0 , \tag{17a}$$

$$\omega_l^{(j)} \bmod 1 \to 0 \tag{17b}$$

hold simultaneously, for some frequencies ω, in the limit of $l \to \infty$. Since Eq. (17a) is a sufficient condition in order to hold Eq. (17b), it suffices to consider Eq. (17a) in testing whether or not the Bragg peak exists. Note that the mod 1 comes from the fact that the argument ω_l enters $\underline{M}_l(\omega)$ through complex exponentials. Note also that Eq. (17a) amounts to stating that the recursion relation of ω_l, i.e.,

$$\omega_{l+1} = n\omega_l + m\omega_{l-1} \bmod 1 , \tag{18}$$

has an asymptotic fixed point located at the origin ($\omega^* = 0$). Equation (18) is a nonlinear iterative map and generally exhibits three qualitatively different behaviors: asymptotic fixed-point, limit-cyclic, and chaotic behaviors.[11] Since the behavior of the map strongly depends on whether or not the characteristic values possess the PV property, let us study the properties of the Fourier spectrum dividing the lattices into three classes.

B. Class I ($n+1>m$)

In this case the characteristic values possess the PV property (i.e., $\tau_+ > 1 > \tau_- > -1$). Writing F_l as $F_l = A_l + B_l$, where A_l (B_l) is the first (second) term in Eq. (6), we have $A_l \simeq F_l$ in the limit of $l \to \infty$. Since B_l goes to zero as $l \to \infty$, A_l approaches to an *integer* F_l or, equivalently,

$$A_l \bmod 1 = F_l \bmod 1 \to 0 \quad \text{as } l \to \infty . \tag{19}$$

Equation (19) is equivalent to stating that Eq. (18) has $\omega^* = 0$. For frequencies ω belonging to the basin of attraction of $\omega^* = 0$, $\underline{M}_l(\omega)$ becomes

$$\begin{bmatrix} n & m \\ 1 & 0 \end{bmatrix} , \tag{20}$$

and thus we have $G_l(\omega) \sim F_l$; i.e., we have Bragg peaks with $\gamma(\omega) = 1$. Noting that Eq. (17a) is equivalent to writing ω as $\omega = s/A_l$ with an integer s, it can be easily shown by using Eqs. (9a) and (9b) that the frequencies belonging to the basin of attraction of $\omega^* = 0$ are given by

$$\omega = \frac{a\tau + b}{m^r(n+m-1)} , \tag{21}$$

where a, b, and r are integers satisfying $0 < \omega < 1$. Note that the region of the frequency to be considered is given by $0 < \omega < 1$ because $G_l(\omega)$ have periodicity of 1, i.e., $G_l(\omega+1) = G_l(\omega)$. We also omit $\omega = 0$, which is a trivial point at which the Fourier amplitude exhibits a Bragg peak regardless of the property of the lattice when $\varepsilon_A + \varepsilon_B \neq 0$. Equation (21) is exactly the same form as what we obtained in the electronic band structure: $\omega = N(E)$.

We confirm the above result by numerical calculation and test the relation between the widths of energy gaps and the strengths of the Fourier-spectral peaks. Figures 4(a) and 4(b) show the absolute values of the Fourier amplitudes for the silver mean and mixed mean ($n = m = 2$) lattices, respectively. In the silver mean lattice, spectral peaks locate at $\omega = (a\tau + b)/2$. Indices (a,b) and the corresponding strengths of the spectral peaks in the figure are in agreement with the locations and widths of the gaps obtained in Sec. II (locations of main gaps are indicated in the upper abscissa of the figure). In the mixed mean lattice, Bragg peaks occur at $\omega = (a\tau + b)/(3\times 2^r)$. Considering the relative strength of spectral peaks, fre-

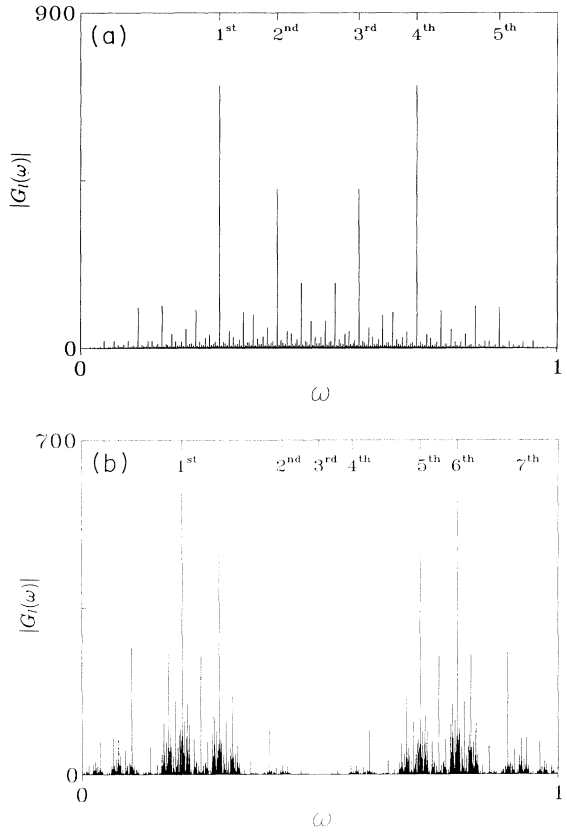

FIG. 4. $|G_l(\omega)|$ vs ω for (a) silver mean and (b) mixed mean lattices. We take $\varepsilon_A = -\varepsilon_B = 1$. The locations and the strengths of the spectral peaks are in a good agreement with those of the IDOS. The upper abscissas represent (a,b)'s of the main gaps.

quencies related to the first, fifth, and sixth main gaps show dominant peaks. Here comes two interesting features of the mixed mean lattice to be mentioned. The first is that the Fourier spectrum exhibits a somewhat blurred structure similar to that of the copper mean lattice (see Fig. 5), even though the lattice is a quasiperiodic one. The blurred structure seems to appear for lattices with $m \neq 1$ regardless of whether the lattice is quasiperiodic or aperiodic. The second is that the Bragg peaks occur at rational values of ω (i.e., $a=0$, $b=3k$) as well as irrational values ($a \neq 0$) even though the characteristic value is irrational (i.e., $\tau=1+\sqrt{3}$), which is in contrast to the ordinary Fibonacci and silver mean lattices.

C. Class II ($n+1=m$)

In this case the characteristic values are $\tau_+=n+1$ and $\tau_-=-1$; it is a marginal case of the PV property. Because of the rational values of $\tau_\pm$, both A_l and B_l are rational: $A_l=2(n+1)^l/(n+2)$ and $B_l=n(-1)^l/(n+2)$. As in class I, we have $F_l \simeq A_l$ in the limit of $l \to \infty$. However, $B_l \bmod 1$ does not go to zero, but has either a two-cyclic value (when $n \neq 2$) or a fixed point value at nonzero (when $n=2$), and so does $A_l \bmod 1$. Thus ω_l in Eq. (18) has no fixed point at the origin, resulting in the absence of Bragg peak. Note that $B_l \bmod 1$ goes to zero with the increase of n such that the Fourier-spectral peaks behave like the Bragg peak. This is quite natural since the limit of $n \to \infty$ means the lattice is in effect a crystal composed of an element A.

As a concrete example, let us consider the copper mean lattice, where

$$\omega_l=\frac{\omega}{3}[2^{l+1}-(-1)^{l+1}], \quad \omega_l^{(1)}=2^l\omega . \tag{22}$$

In this case the recursion relation becomes

$$\omega_{l+1}=\omega_l+2\omega_{l-1} \bmod 1 , \tag{23a}$$

$$\omega_{l+1}^{(1)}=2\omega_l^{(1)} \bmod 1 . \tag{23b}$$

Equation (23b) has a fixed point at the origin for frequencies $\omega=m/2^r$, where m and r are integers satisfying $0<\omega<1$. However, at these values of ω, Eq. (23a) has no fixed point, but has two-cyclic values $\pm\tilde{\omega}$ [see Eq. (34)]. This indicates that there is no frequency making both ω_l and $\omega_l^{(1)}$ go to zero simultaneously, which in turn implies the absence of a Bragg peak. The scaling exponent $\gamma(\omega)$ can be easily determined for frequencies giving rise to *any* limit-cyclic behavior of the recursion relations. For example, for $\omega=m/2^r$, $\underline{M}_l(\omega)$ becomes two-cyclic with

$$\underline{M}_l^{\pm}(\omega)=\begin{bmatrix} 1 & 1+e^{+2\pi i\tilde{\omega}} \\ 1 & 0 \end{bmatrix} . \tag{24}$$

And $\gamma(\omega)$ can be determined by the largest eigenvalue of the second iterate of $\underline{M}_l(\omega)$, $\underline{M}_l^{[2]}(\omega)=\underline{M}_l^{+}(\omega)\underline{M}_l^{-}(\omega)$. See Sec. IV B for the detailed calculation.

Figure 5 shows the absolute values of the Fourier amplitudes for the copper mean lattice. The global structure differs from that of the silver mean lattice; it shows clustering behaviors, and inside the clusters there exist

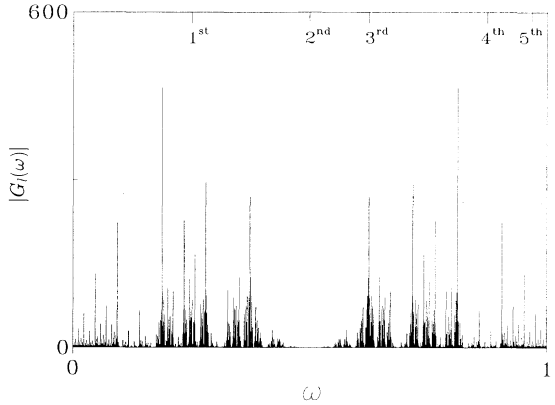

FIG. 5. $|G_l(\omega)|$ vs ω for the copper mean lattice. We take $\varepsilon_A=-\varepsilon_B=1$. The global structure shows different behaviors from that of the silver mean lattice.

blurred structures of densely packed peaks. Dominant peaks locate at wave numbers satisfying $\omega=3k/2^r$ with integers k and r. Thus, of the frequencies related to the main gaps by $\omega=N(E)$, the only frequency related to the third main gap shows a dominant peak, while all the other frequencies show negligibly small peaks; the dominant spectral peaks are not directly related to the widths of the main gaps. This is a distinctive feature from the case of the silver mean lattice. Note that, despite the discrepancy between the strengths of the spectral peaks and the widths of the energy spectral gaps, one can obtain the locations and scaling behaviors of the dominant spectral peaks. This is treated in detail in Sec. IV for the copper mean lattice.

D. Class III ($n+1<m$)

In this case the characteristic values possess no PV property (i.e., $\tau_+>1$ and $\tau_-<-1$). Moreover, $B_l \bmod 1$ does not converge to a fixed point or to a limit cycle value unlike the previous two classes and so does $A_l \bmod 1$. This implies the absence of a Bragg peak. Furthermore, because of the chaotic behavior in Eq. (18), it is difficult to define a frequency at which the spectral peak has a well-defined scaling exponent $\gamma(\omega)$.

Figure 6 shows the absolute values of the Fourier amplitudes for the nickel mean lattice. As in the copper mean lattice, the global structure looks blurred. Moreover, all the frequencies related to the main energy spectral gaps have negligibly small peaks. Comparing with the case of the copper mean lattice, one can see that the strength of the dominant peaks reduces considerably, which suggests that the nickel mean lattice is more disordered than the copper mean lattice. Note that, even though the location of the dominant peaks does not coincide with that of the main gaps, the generic expression for the location of the spectral peaks is given by $\omega=(a\tau+b)/3^r$, which is of the same form as Eq. (10) with $n=1$ and $m=3$. Thus it can be said that the Fourier-spectral peaks locate at frequencies $\omega=N(E)$ as in the previous two classes, while the strength of the peak is irrelevant to the width of the energy spectral gap.

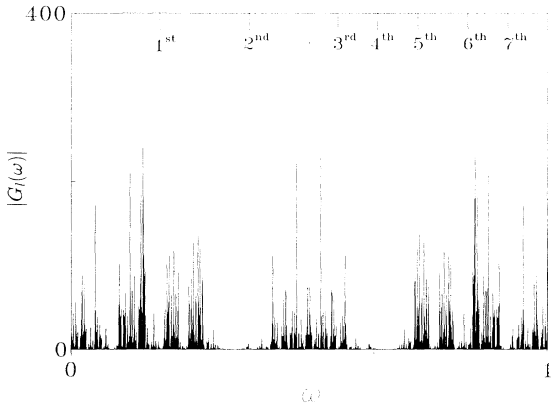

FIG. 6. $|G_l(\omega)|$ vs ω for the nickel mean lattice. We take $\varepsilon_A=-\varepsilon_B=1$. The global structure shows similar behavior to that of the copper mean lattice.

Note also that the scaling indices, in a weak sense, of the Fourier-spectral peaks of a lattice belonging to class III may take diverse values less than unity, which implies that the spectral peaks are a multifractal object. In fact, the authors in Ref. 29 have performed a multifractal analysis on the Fourier spectra of the copper mean and nickel mean lattices to find the multifractality in them; Fourier-spectral measures of lattices with $n+1\leq m$ are considered to be singular continuous ones.

IV. COPPER MEAN LATTICE WITH VARIOUS INITIAL CONDITIONS

In this section we consider the copper mean lattice in detail, with varying the initial conditions of Eq. (2). Before going on, a few remarks should be mentioned. The first is that, since the lattice is an example of aperiodic lattices, the study will shed some insight into the properties of deterministic aperiodic lattices. The second is that the lattice is tractable analytically because the characteristic value is a rational value ($\tau=2$), which is a common feature of the lattices with $n+1=m$. The third and the most important remark lies in the relation between the two lattices, the *period-doubling*[12,18,25] and the *ordinary* copper mean lattices.

The period-doubling lattice is defined by the substitution rule $\{A\rightarrow AB, B\rightarrow AA\}$ starting with the letter A. The lattice with a potential given by the period-doubling sequence is known to be quasiperiodic,[12] and the energy spectrum is known to be a singular continuous one supported on a Cantor set of zero Lebesgue measure for all nonzero values of the potential strength.[18] Meanwhile, the lattice with a potential given by the ordinary copper mean sequence, generated by the rule $\{A\rightarrow ABB, B\rightarrow A\}$, contains no Bragg peak as shown in the previous section, and the energy spectrum contains smooth parts with extended electronic states as well as singular continuous parts with critical electronic states.[23,27,31] However, it can be easily checked that the two lattices are generated by a stacking rule $S_{l+1}=S_lS_{l-1}^2$ with different initial conditions. In fact, the ordinary copper mean sequence becomes identical with the period-doubling sequences when the cluster BB is replaced by B. Then why do the two lattices have difficult properties, and what is the reason for the differences? Can the properties of the lattices be described in a unique way? This stimulates us to study the copper mean lattice with different initial conditions. To this end, of the various possibilities in the choice of the initial conditions, we choose the initial conditions with $S_1=\{A\}$ and $S_2=\{AB^p\}$, where p is a positive integer. In this circumstance the period-doubling sequence corresponds to $p=1$ and the ordinary copper mean sequence to $p=2$. Note that any lattice with $p\geq 3$ has no substitution rule associated with the sequence; it can only be defined by the stacking rule with a specific p. The existence of the substitution rule implies the existence of full inflation-deflation symmetry, and thus the cases of $p=1$ and 2 have the symmetry, while the cases of $p\geq 3$ do not. As can be seen in the following, the global structures of the energy spectrum and the Fourier spectrum maintain regardless of p, which reveals that the stacking rule may be more fundamental than the substitution rule in classifying deterministic aperiodic lattices.

A. IDOS

The constructing elements of the lattice, in the limit of the large potential strength, are given by $\{B^p, A, A^3\}$. The numbers of constructing elements and the total number of elements in the lth generational sequence are given by

$$N_{B^p}^l=F_{l-2}\ ,\quad N_A^l=2F_{l-4}\ ,\quad N_{A^3}^l=F_{l-3}\ , \tag{25a}$$

$$N_l=pN_{B^p}^l+N_A^l+3N_{A^3}^l=F_l+(p-2)F_{l-2}\ . \tag{25b}$$

The number of the global subbands is $(p+3)$; p subbands come from the element B^p, and three subbands come from the "monatomic" element A and the "triatomic" elements A^3. Note that, in the lowest order of the approximation, the energy of the monatomic element and one of the three energies of the triatomic element are degenerate, and thus the number of global subbands is not $(p+4)$ but $(p+3)$. From this fact one can write the branching rule of the global subbands as

$$N_l\rightarrow F_{l-2}+\cdots+F_{l-2}+F_{l-3}+F'_{l-2}+F_{l-3}\ . \tag{26}$$

Here F'_{l-2} $(=F_{l-3}+2F_{l-4})$ represents the number of eigenvalues of the degenerate subband. In obtaining the branching rules in the following hierarchies, one can treat each subband independently to others as in the case of the ordinary Fibonacci lattice. The decomposition produces two kinds of lattices. Both the p subbands coming from the element B^p and the two subbands coming from the element A^3 are described by an F-type lattice where two kinds of modified hopping parameters $\{T'_A, T'_B\}$ are arranged in the ordinary copper mean sequence while the degenerate subband is described by an F'-type lattice where two kinds of modified site energies $\{V'_A, V'_B\}$ are arranged in the ordinary copper mean sequence. Thus one can deduce that the branching rules at any hierarchy are given by[26]

$$F_i \rightarrow F_{i-2}+F'_{i-1}+F_{i-2} , \tag{27a}$$

$$H_i \rightarrow \begin{cases} F_{i-2}+F_{i-2}+F_{i-3}+F'_{i-2}+F_{i-3} \\ \text{or} \\ F_{i-3}+F'_{i-2}+F_{i-3}+F_{i-2}+F_{i-2} . \end{cases} \tag{27b}$$

These results reveal that the branching rules of sub-subbands are independent of the initial condition; the copper mean lattices have a fractal structure regardless of the integer p.

As in Sec. II, we determine the IDOS $N(E)$ and thus characterize the location of energy spectral gaps. Since we have the relations $F_{l-2}/N_l=1/(p+2)$ and $F_{l-3}/N_l=1/[2(p+2)]$ in the limit of $l\rightarrow\infty$, the density of states on any global subband has one of the two values $\{1/(p+2),\ 1/[2(p+2)]\}$. Furthermore, because each subband at any hierarchy has one of $\{F_{l-r},F_{l-r-1}\}$ eigenvalues, the IDOS at any hierarchy can be written as

$$N(E)=\frac{k}{2^r(p+2)} , \tag{28}$$

with integers k and r. This is a gap labeling rule for the copper mean lattice. Thus, by setting $\omega=N(E)$, one can expect that the Fourier-spectral peaks may occur at frequencies given by

$$\omega=\frac{k}{2^r(p+2)} . \tag{29}$$

Note that the integer p is included in the denominator of Eq. (29), which plays an important role in illustrating why the Fourier spectra of the period doubling and the ordinary copper mean lattices exhibit different behaviors.

B. Fourier spectrum

The recursion relation of the Fourier amplitudes is given by Eq. (15), where

$$\underline{M}_l(\omega)=\begin{bmatrix} 1 & e^{2\pi i\omega_l}+e^{2\pi i\omega_l^{(1)}} \\ 1 & 0 \end{bmatrix} \tag{30}$$

and

$$\omega_l=N_l\omega=\tfrac{1}{3}[(p+2)2^{l-1}-(p-1)(-1)^{l-1}]\omega , \tag{31a}$$

$$\omega_l^{(1)}=(N_l+N_{l-1})\omega=(p+2)2^{l-2}\omega . \tag{31b}$$

For frequencies in Eq. (29), $\omega_l^{(1)} \bmod 1$ goes to zero while $\omega_l \bmod 1$ does not. Thus $\gamma(\omega)$ is less than unity and there is no Bragg peak. The only exceptional case is when $p=1$. In this case the second term of Eq. (31a) vanishes, and both $\omega_l^{(1)} \bmod 1$ and $\omega_l \bmod 1$ go to zero simultaneously for frequencies in Eq. (29). Thus Bragg peaks occur at these frequencies.

For frequencies ω satisfying Eq. (29), ω_l and $\omega_l^{(1)}$ become

$$\omega_l=\frac{k}{3}2^{l-r-1}+(-1)^l\omega' , \quad \omega_l^{(1)}=2^{l-r-2}k , \tag{32}$$

where

$$\omega'=\frac{1}{3}\left[\frac{p-1}{p+2}\right]\frac{k}{2^r} . \tag{33}$$

As l increases, $\omega_l^{(1)} \bmod 1$ goes to zero while $\omega_l \bmod 1$ takes two-cyclic values $\tilde{\omega}_1$ and $\tilde{\omega}_2$, where

$$\tilde{\omega}_1=\frac{k}{3}+(-1)^{r+1}\omega' , \quad \tilde{\omega}_2=\frac{2k}{3}-(-1)^{r+1}\omega' . \tag{34}$$

Thus $\underline{M}_l(\omega)$ becomes two-cyclic, and the eigenvalues $\lambda_\pm$ of the second iterate of $\underline{M}_l(\omega)$ become

$$\lambda_\pm=\tfrac{1}{2}(3+2\cos\tilde{\omega}\pm|1+2\cos\tilde{\omega}|) , \tag{35}$$

where $\tilde{\omega}$ is one of the values $\tilde{\omega}_1$ and $\tilde{\omega}_2$ which satisfies $0<\tilde{\omega}<\frac{1}{2}$. The scaling exponent $\gamma(\omega)$ then becomes

$$\gamma(\omega)=\frac{\ln|\lambda_+|}{2\ln\tau}=\begin{cases} \ln(2+2\cos\tilde{\omega})/(2\ln 2) , & 0<\tilde{\omega}<\frac{1}{3} \\ 0 , & \frac{1}{3}\le\tilde{\omega}<\frac{1}{2} . \end{cases} \tag{36}$$

Note that the scaling exponent $\gamma(\omega)$ for a frequency ω which makes $\underline{M}_l(\omega)$ any limit cyclic can also be determined in a similar way.[26] Now let us consider three examples ($p=1,2,3$) of the lattices explicitly.

1. $p=1$ case

In this case both ω_l and $\omega_l^{(1)}$ satisfy similar recursion relations, i.e.,

$$\omega_{l+1}=2\omega_l \bmod 1 , \tag{37a}$$

$$\omega_{l+1}^{(1)}=2\omega_l^{(1)} \bmod 1 . \tag{37b}$$

When $k=3s$ in Eq. (29), Eqs. (37a) and (37b) have a fixed point at the origin simultaneously, and the corresponding peaks have a scaling exponent $\gamma(\omega)=1$. Meanwhile, when $k=3s\pm1$ in Eq. (29), Eqs. (37a) and (37b) have a fixed point at $\tilde{\omega}=\frac{1}{3}$, and thus $\gamma(\omega)=0$.

Figure 7 shows the absolute values of the Fourier amplitudes. As can be seen clearly in the figure, the global structure looks cleaner than that of Fig. 5; the spectrum consists of Bragg peaks at $\omega=s/2^r$, where s is an odd in-

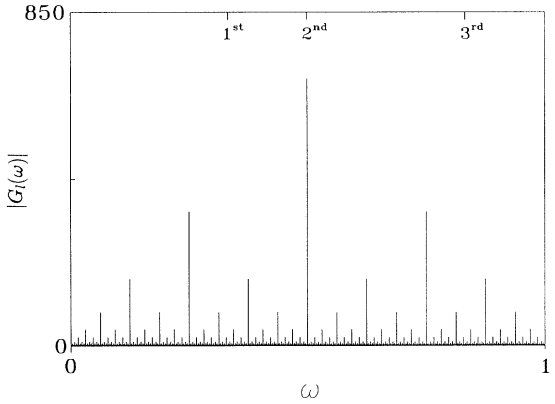

FIG. 7. $|G_l(\omega)|$ vs ω of the period-doubling lattice ($p=1$). We take $\varepsilon_A=-\varepsilon_B=1$. The global structure shows sharp Bragg peaks. Compare it with Fig. 5.

teger satisfying $0<\omega<1$. Thus the lattice can be said to be quasiperiodic. However, the relation between the IDOS and Fourier spectrum is unlike the standard quasiperiodic lattices. From Eqs. (25b) and (26), one can obtain that the three mean energy spectral gaps are characterized by $N(E)=\frac{1}{3}$, $\frac{1}{2}$, and $\frac{5}{6}$. Figure 8 confirms this result. Considering the following hierarchies, one can find the gaps are characterized by $N(E)$ whose denominator is 3 times a power of 2. But the frequency ω having the Bragg peak has a denominator not 3 times a power of 2, but a power of 2. Especially, of the frequencies related to the main gaps, only the frequency corresponding to the second main gap has a Bragg peak, while the other two have peaks negligibly small. Thus the period-doubling lattice shows similar behavior to that aperiodic lattices exhibit, even though the lattice contains Bragg peaks. This strongly reveals that the period-doubling lattice is an exceptional case of aperiodic lattices.

2. $p=2$ case

In this case the two recursion relations are given by

$$\omega_{l+1}=\omega_l+2\omega_{l-1} \bmod 1 , \tag{38a}$$

$$\omega_{l+1}^{(1)}=2\omega_l^{(1)} \bmod 1 . \tag{38b}$$

The frequencies in Eq. (29) are in the basin of attraction at zero in Eqs. (38b) and show two-cyclic behavior $(\tilde{\omega},-\tilde{\omega})$ in Eq. (38a) with

$$\tilde{\omega}=\begin{cases}(F_{r+1}\mp s)/2^{r+2} & \text{if } k=3s-1 ,\ s=2,4,6,\ldots , \\ s/2^{r+2} & \text{if } k=3s ,\ s=1,3,5,\ldots , \\ (F_{r+1}\pm s)/2^{r+2} & \text{if } k=3s+1 ,\ s=0,2,4,\ldots ,\end{cases} \tag{39}$$

where the upper (lower) sign corresponds to an even (odd) integer of r. Thus $\underline{M}_l(\omega)$ becomes two-cyclic. Of the frequencies giving rise to two-cyclic behaviors of $\underline{M}_l(\omega)$, those satisfying the condition $k=3s$ exhibit dominant peaks as in the $p=1$ case. This behavior can be easily understood by considering the periodic approximant of the infinite lattice. In the lth periodic approximation, the allowed values of ω become s/F_l, where s is an integer. Since F_l can be written as $F_l\simeq 2^{l+1}/3$ for large l, one can write $\omega\simeq 3s/2^{l+1}$, which goes to two-cyclic values $\tilde{\omega}=s/2^{l+1}$ after appropriate iterations. Note that, as shown in the previous section, locations of the Fourier-spectral peaks correspond to those of the energy spectral gaps even though the strengths of the dominant peaks do not.

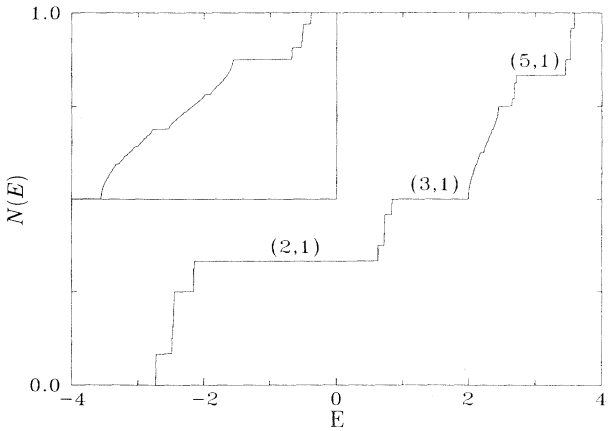

FIG. 8. IDOS vs E for the period-doubling lattice. The systems size is $N=1024$ ($l=11$). We take $V=V_A=-V_B=2$ and $T=1$. The IDOS is characterized by (k,r) where $N(E)=k/(3\cdot 2^r)$. The inset represents the third main subband which is a mixed subband of monatomic (A) and triatomic (A^3) elements. The shape of the IDOS looks like that of crystal, i.e., looks smoothlike.

3. $p=3$ case

In this case the frequencies in Eq. (29) make $\omega_l^{(1)}$ mod 1 go to zero while making ω_l mod 1 go to two-cyclic values $\pm\tilde{\omega}$ with

$$\tilde{\omega}=\begin{cases}s/(5\times 2^{r-2}) , & k=3s , \\ [N_{r+1}\mp(s\pm 1)(-1)^{r+1}]/(5\times 2^{r-2}) , & \\ & k=3s\pm 1 .\end{cases} \tag{40}$$

Of the frequencies giving rise to two-cyclic behavior of $\underline{M}_l(\omega)$, those satisfying $k=3s$ give dominant spectral peaks as in the previous two cases. Since the five main energy spectral gaps are located at $N(E)=\frac{1}{5}$, $\frac{2}{5}$, $\frac{3}{5}$, $\frac{7}{10}$, and $\frac{9}{10}$, the frequencies ω related to the third and fifth main gaps have dominant peaks, while the others have not. As in the previous two cases, locations of the Fourier-spectral peaks correspond to those of the energy spectral gaps, while the strengths of the dominant spectral peaks do not.

From the above study, we obtain that dominant spectral peaks occur when the condition $k=3s$ in Eq. (29) holds. When $k\neq 3s$, the corresponding spectral peaks generically have small, but not zero, values of $\gamma(\omega)$. Thus the global structure exhibits a blurred behavior. The only exception is in the case of $p=1$, where $\gamma(\omega)$ equals exactly zero for $k\neq 3s$. This is the reason why dominant spectral peaks in the period-doubling lattice look isolated.

The global structure of the Fourier spectrum depends on the initial condition p. We find that the structure becomes more blurred and thus more disordered with the increase of p. This can be understood by considering the following two facts. The first is that the minimum value of $\gamma(\omega)$ of dominant peaks decreases with the increase of p, e.g., $\gamma(\frac{3}{8})\simeq 0.8858$ for $p=2$, $\gamma(\frac{3}{10})\simeq 0.6942$ for $p=3$, and so forth. The second is that some spectral peaks occurring at $k\neq 3s$ can have scaling exponents which are comparable with those of spectral peaks occurring at $k=3s$.

The two-point correlation function of the sequence, which is related to the Fourier intensity measure of the sequence,[34] clearly reveals the blurred structure. Figure 9 shows the partial correlation functions $C_N(r)$ for (a) $p=1$, (b) $p=2$, and (c) $p=3$, where

$$C_N(r)=\frac{1}{N}\sum_{k=1}^{N}\varepsilon_k\varepsilon_{k+r} . \tag{41}$$

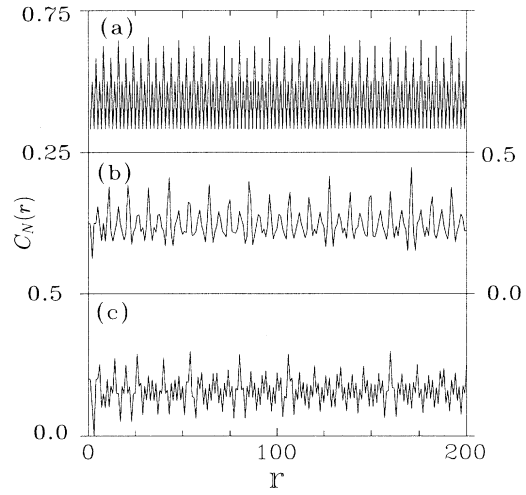

FIG. 9. Partial correlation functions of the copper mean sequence with (a) $p=1$, (b) $p=2$, and (c) $p=3$. We take $\varepsilon_A=1$ and $\varepsilon_B=0$.

As can be clearly seen, the correlation becomes weaker with the increase of p.

C. Electronic states

The trace map method has been used as a powerful tool in examining electronic properties of substitutional lattices. The method makes it easy to calculate the energy spectrum and to study the behaviors of electronic states at any generational sequence of a given lattice. Thus, using the method, we examine electronic states of the copper mean lattice with varying initial conditions. To this end, one can write Eq. (3) as

$$\begin{bmatrix}\psi_{n+1}\\ \psi_n\end{bmatrix}=\underline{M}(n)\begin{bmatrix}\psi_n\\ \psi_{n-1}\end{bmatrix}=\underline{M}^{(n)}\begin{bmatrix}\psi_1\\ \psi_0\end{bmatrix}, \tag{42}$$

where $\underline{M}(n)$ and $\underline{M}^{(n)}$ are defined by

$$\underline{M}(n)=\begin{bmatrix}(E-V_n)/T & -1\\ 1 & 0\end{bmatrix}, \tag{43a}$$

$$\underline{M}^{(n)}=\underline{M}(n)\underline{M}(n-1)\cdots\underline{M}(2)\underline{M}(1)\ . \tag{43b}$$

From now on, we take the hopping parameter T to be unity. By using Eq. (2), the recursion relation of the transfer matrix $\underline{M}_l$ ($\equiv\underline{M}^{(N_l)}$) can be written as

$$\underline{M}_{l+1}=\underline{M}_{l-1}^2\underline{M}_l\ , \tag{44}$$

and thus the trace map of the copper mean lattice is given by

$$x_{l+1}=x_l(4x_{l-1}^2-2)-\Delta\ ,\quad \Delta=\tfrac{1}{2}\mathrm{tr}(\underline{M}_{l-1}^{-2}\underline{M}_l)\ , \tag{45}$$

where $x_l\equiv\frac{1}{2}\mathrm{tr}(\underline{M}_l)$. Note that the quantity Δ is an l-independent quantity (i.e., $\Delta_{l+1}=\Delta_l$) and depends on the initial conditions of the stacking rule. Since $\underline{M}_1=\underline{M}_A$ and $\underline{M}_2=\underline{M}_B^p\underline{M}_A$, where

$$\underline{M}_A=\begin{bmatrix}E-V_A & -1\\ 1 & 0\end{bmatrix},\quad \underline{M}_B=\begin{bmatrix}E-V_B & -1\\ 1 & 0\end{bmatrix}, \tag{46}$$

one can write the invariant Δ as $\Delta=\frac{1}{2}\mathrm{tr}(\underline{M}_1^{-2}\underline{M}_2)$. Now, for a unimodular matrix $\underline{M}$, one can write a power of $\underline{M}$ as

$$\underline{M}^p=C_p(m)\underline{M}-C_{p-1}(m)\underline{I}\ . \tag{47}$$

Here $\underline{I}$ is the unit matrix and $C_p(m)$ is a polynomial of $m\equiv\mathrm{tr}(\underline{M})$ (the Chebychev polynomial of the second kind), which satisfies the recursion relation

$$C_{p+1}(m)=mC_p(m)-C_{p-1}(m)\ , \tag{48}$$

with $C_0(m)=0$ and $C_1(m)=1$. Using Eq. (47), the invariant becomes

$$\Delta=C_p(m_B)-\tfrac{1}{2}m_AC_{p-1}(m_B)\ , \tag{49}$$

where $m_{A(B)}=\mathrm{tr}(\underline{M}_{A(B)})=E-V_{A(B)}$.

An energy E corresponding to a point x_l that does not escape to infinity in the iteration of Eq. (45) belongs to the energy spectrum. In general, the wave function of a state corresponding to a periodic orbit in trace space exhibits self-similarity, while the wave function corresponding to an aperiodic orbit exhibits chaotic behavior. Since such critical states have been illustrated many times in the literature,[20,22,26,27,30] we focus our attention on the possible existence of extended states and on the related property, i.e., the state transition whose definition is, according to Zhong *et al.*,[27] the transition from the local density of states with a smooth behavior in some energy regions to another one without any smooth part. The possible existence of the state transition provides a reason why the study of the extended state is important.

Because of the stacking rule of the sequence, the copper mean lattice in the infinite limit of the system size can be thought as a mixture of two kinds of unit cells S_i^2 and S_{i+1}. Let us call the unit cell S_i^2 an *impurity* embedded in a *crystal* composed of unit cells with cell size S_{i+1}. Assume that an electron travels the impurity without any resistance for a certain energy E. In terms of the transfer matrix, this amounts to $\underline{M}_i^2\propto\underline{I}$. Then the electron can also travel the whole lattice without any resistance if the energy E is in the energy spectrum E' of the crystal, and thus the corresponding electronic state is *extended* through the whole size of the lattice. We call this state the *resonant state,* since the characteristic of the state comes from the resonance condition between the impurity and crystal. Now let us consider specific examples ($p=1,2,3$) and study the possible existence of the resonant state together with the state transition.

1. $p=1$ case

The sequence is given by

$$A\to AB\to AB\underline{AA}\to AB\underline{AA}\,AB\,AB\to AB\underline{AA}\,AB\,AB\,AB\underline{AA}\,AB\underline{AA}$$
$$\to AB\underline{AA}\,AB\,AB\,AB\underline{AA}\,AB\underline{AA}\,AB\underline{AA}\,AB\,AB\,AB\underline{AA}\,AB\,AB\to\cdots$$

and the invariant by

$$\Delta=1 \ . \tag{50}$$

One can see from Eq. (45) that if an energy E satisfies the condition $x_l=0$, then the relations

$$x_{l+1}=-1 \quad \text{and} \quad x_{l+m}=1 \tag{51}$$

hold for all $m \geq 2$. Noting that the condition $x_l=0$ is equivalent to $\underline{M}_l^2=-\underline{I}$ since $\underline{M}_l$ is unimodular, it suffices to consider whether or not an energy satisfying the condition $x_l=0$ belongs to the allowed energy E' of the crystal.

First of all, it can be easily shown that the energy $E=V$ $(=V_A=-V_B)$ satisfies $x_1=0$. Thus the lattice can be regarded as a binary crystal, called the AB crystal, with impurities AA (underlined letters in the above sequence). But the allowed energy of the AB crystal is $E'=\pm(V^2-4\cos^2 q)^{1/2}$, where $q(=2\pi\omega)$ is an incident wave vector, and thus the state with the energy $E=V$ is just the edge state of the upper subband of the AB crystal; it is a resonant state. It can be also found that the energy $E=\pm(V^2+2)^{1/2}$ satisfies $x_2=0$, and the corresponding state is the resonant state satisfying the resonance condition between the impurity $ABAB$ and the crystal with a unit cell $ABAA$. Similarly, a state with an energy satisfying $x_3=0$ is a resonant state between the impurity $ABAAABAA$ and the crystal with a unit cell $ABAAABAB$.

It should be noted that Δ is independent of the potential parameter V such that the resonant states always exist independent of V. Thus there is no state transition, and the smooth parts of the energy spectrum always exist regardless of V. This is clearly shown in Fig. 8. The IDOS in the figure is obtained for $V=2$. The resonant states with energies $E=2$ and $\sqrt{6}$ belong to the third main subband in the figure, which is magnified in the inset of the figure. The smooth parts, i.e., Bloch-like parts of the energy spectrum near $E=2$ and $\sqrt{6}$, are clearly seen. Compare it with the inset of Fig. 2, which corresponds to the $p=2$ case. The IDOS in Fig. 2 is obtained for the same parameter as in Fig. 8, but as shown in the following, there is no resonant state for the potential parameter and the shape of the inset looks different from that of Fig. 8.

2. $p=2$ case

The sequence is given by

$$A \rightarrow ABB \rightarrow ABB\underline{AA} \rightarrow ABB\underline{AA}\,ABB\,ABB \rightarrow ABB\underline{AA}\,ABB\,ABB\,ABB\underline{AA}\,ABB\underline{AA} \rightarrow \cdots$$

and the invariant by

$$\Delta=\tfrac{1}{2}(2m_B-m_A) \ . \tag{52}$$

Unlike the $p=1$ case, Δ depends on both V and E and is equal to unity only if E and V satisfy the condition $2m_B-m_A=2$.

For $E=-V$, we have $\Delta=V$ and $\underline{M}_B^2=-\underline{I}$, from which the cluster BB can be regarded as an impurity embedded in a crystal with a unit cell A, called the A crystal. The allowed energies of the A crystal are given by $E'=V+2\cos q$. Thus it can be easily deduced that the energy $E=-V$ belongs to E' only for $V \leq 1$, and the corresponding state is extended. For $V>1$, x_l is not bounded and the state is no longer extended in a common sense. Thus the state transition occurs at $V=1$, which is a different feature from that of the $p=1$ case.

For $E=V$, we have $\Delta=2V$ and $\underline{M}_A^2=-\underline{I}$; the cluster AA (underlined letter in the above sequence) is regarded as an impurity embedded in a crystal with a unit cell ABB, called the ABB crystal. In this case, x_l is bounded and the corresponding state is extended only for $V \leq \frac{1}{2}$; the state transition occurs at $V=\frac{1}{2}$. Figure 2 shows the IDOS obtained for $V=2$, and for this value of the potential parameter there is no extended state unlike the $p=1$ case. The inset of the figure represents the fourth main subband. Comparing it with that of Fig. 8, one can find how the existence of the resonant states affect the feature of the IDOS.

One can also find resonant states even for $E \neq \pm V$. From the condition $2m_B-m_A=2$, it is possible to write $x_2=m_B^3-m_B^2-m_B+1$. Thus, for an energy E with $x_2=0$, the lattice can be thought as a mixture of the impurity ABB and a crystal with a unit cell $ABBAA$, and the corresponding state is a resonant state. We find numerically that the parameters are given by $V \simeq 0.376\,512\ldots$ and $E \simeq 0.870\,466\ldots$.

3. $p=3$ case

The sequence is given by

$$A \rightarrow ABBB \rightarrow ABBB\underline{AA} \rightarrow ABBB\underline{AA}\,ABBB\,ABBB \rightarrow ABBB\underline{AA}\,ABBB\,ABBB\,ABBB\underline{AA}\,ABBB\underline{AA} \rightarrow \cdots$$

and the invariant by

$$\Delta=\tfrac{1}{2}m_B(2m_B-m_A)-1 \ . \tag{53}$$

For $E=V$, we have $\Delta=4V^2-1$ and $\underline{M}_A^2=-\underline{I}$; the lattice is a mixture of the impurity AA and the crystal with a unit cell $ABBB$, called the $ABBB$ crystal. The corresponding state is extended only for $V \leq 1/\sqrt{2}$, and the state transition occurs at $V=1/\sqrt{2}$.

The results obtained above indicate that the state transition generally occurs when the invariant Δ depends on the potential parameter V. In the case of $p=1$, resonant states exist for all strength of V and no state transition

occurs. But when $p \neq 1$, Δ depends on V such that the state transition occurs at certain value of V. It should be noted that the importance of the possible existence of resonant states lies in that the energy spectrum shows a qualitatively different feature depending on whether or not there exist resonant states.

Before ending this section, it should be mentioned that the resonance condition is one of mechanisms for the existence of extended states in aperiodic lattices. The same kind of resonance condition occurring in the copper mean lattice can be observed in various lattices such as the modified Fibonacci,[37,38] prime-number,[39] Thue-Morse,[14] and random dimer[40] lattices. In fact, it turns out that the resonant states in the random dimer lattice play a crucial role in the dynamics of the wave packet. It is well known that, when a lattice consists of random potentials, all the electronic states are localized exponentially such that the wave packet does not propagate the lattice. However, in the random dimer lattice, electronic states around a resonant state have localization lengths large enough which can overcome the whole lattice size such that the propagation of the wave packet, i.e., diffusion of the wave packet, can be possible. A similar situation may occur in the prime-number lattice since electronic states are similar to those of the random dimer lattice. In the ordinary Fibonacci lattice, the diffusion index decreases continuously with the increase of V. A similar situation may occur in the copper mean lattice because most of the allowed states are considered to be critical. However, the resonant states and the state transition may play a role in characterizing the diffusion behavior which may be different from the behavior of a system which has no resonant state.

V. SUMMARY

In this paper we studied the electronic and Fourier-spectral properties of the one-dimensional GF lattices.

Using the idea of an approximated RG scheme, we obtained the generalized gap labeling rule of the GF lattices. Locations of gaps are wholly characterized by the characteristic value. The existence of the gap labeling rule, regardless of whether a given lattice is quasiperiodic or aperiodic, seems to be due to the existence of self-similarities in the sequence structure.

Through the recursion relations of Fourier amplitudes, Fourier-spectral properties of the GF lattices were studied. The global structure of the Fourier spectrum shows different behaviors depending on whether or not the characteristic values possess the PV property. In a lattice with $n+1>m$, not only the location but also the strength of the Fourier-spectral peak is in agreement with the energy spectral gap; the dominant spectral peak corresponds to the dominant gap. In a lattice with $n+1 \leq m$, however, only the location of the spectral peak coincides with that of the energy spectral gap, while the strength of the spectral peak is irrelevant to the hierarchy of the band structure. In connection with these facts, it should be mentioned that Luck[12] predicted that a strong enough singularity in the Fourier intensity of a lattice generates a spectral gap. Our result in the lattice with $n+1>m$ coincides well with this prediction. However, when $n+1 \leq m$, the prediction does not hold. But there is no inconsistency between the two results, since the limits of the strength of V are different from each other; Luck considered the limit of $V \rightarrow 0$, while we considered the limit of $V \rightarrow \infty$.

The influences of initial conditions in constructing a desired lattice on the electronic and Fourier-spectral properties were studied through the detailed investigation of the copper mean lattice. It was found that the fractal structure of the energy spectrum is independent of the initial conditions, while local electronic properties depend on the initial conditions. There exist resonant states which contribute to the smooth, or Bloch-like, part of the energy spectrum. The state transition generally occurs when the invariant Δ depends on the potential parameter V. The initial conditions also have an influence on the global structure of the Fourier spectrum. The global structure becomes more blurred with the increase of p. An exceptional example is the case of $p=1$, where Bragg peaks exist. However, even in this case, the relation between the IDOS and Fourier spectrum looks like that of aperiodic lattices ($p \neq 1$).

ACKNOWLEDGMENT

This work is supported in part by the Center for Theoretical Physics, Seoul National University.

[1]M. Kohmoto, L. P. Kadanoff, and C. Tang, Phys. Rev. Lett. **50**, 1870 (1983); S. Ostrund, R. Pandit, D. Rand, H. J. Schellnhuber, and E. Siggia, *ibid.* **50**, 1873 (1983).
[2]A. Sütö, J. Stat. Phys. **56**, 525 (1989).
[3]Q. Niu and F. Nori, Phys. Rev. Lett. **57**, 2057 (1986).
[4]Y. Liu and W. Sritrakool, Phys. Rev. B **43**, 1110 (1991).
[5]J. M. Luck and D. Petritis, J. Stat. Phys. **42**, 289 (1986); Y. Liu, X. Fu, W. Deng, and S. Wang, Phys. Rev. B **46**, 9216 (1992).
[6]E. Bombieri and J. E. Taylor, J. Phys. (Paris) Colloq. **47**, C3-19 (1986).
[7]D. Shechtman, I. Blech, D. Gratias, and J. W. Cahn, Phys. Rev. Lett. **53**, 1951 (1984).
[8]L. Esaki, Int. J. Mod. Phys. B **3**, 487 (1989), and references therein.
[9]F. Axel, J. P. Allouche, M. Kléman, M. Mendès-France, and J. Peyrière, J. Phys. (Paris) Colloq. **47**, C3-181 (1986).
[10]R. Riklund, M. Severin, and Y. Liu, Int. J. Mod. Phys. B **1**, 121 (1987).
[11]Z. Cheng and R. Savit, Phys. Rev. B **37**, 4375 (1988); J. Stat. Phys. **60**, 383 (1990).
[12]J. M. Luck, Phys. Rev. B **39**, 5834 (1989).
[13]C. Godrèche and J. M. Luck, J. Phys. A **23**, 3769 (1990).
[14]C. S. Ryu, G. Y. Oh, and M. H. Lee, Phys. Rev. B **46**, 5162 (1992); Phys. Rev. B **48**, 132 (1993).
[15]D. Huang, G. Gumbs, and M. Kolář, Phys. Rev. B **46**, 11 479 (1992).

[16]S. Aubry, C. Godrèche, and J. M. Luck, J. Stat. Phys. **51**, 1033 (1988).
[17]M. Dulea, M. Johansson, and R. Riklund, Phys. Rev. B **45**, 105 (1992); **46**, 3296 (1992).
[18]J. Bellissard, A. Bovier, and J. M. Ghez, Commun. Math. Phys. **135**, 379 (1991).
[19]H. E. Roman, Phys. Rev. B **36**, 7173 (1987); G. Y. Oh, C. S. Ryu, and M. H. Lee, *ibid.* **45**, 6400 (1992).
[20]G. Gumbs and M. K. Ali, Phys. Rev. Lett. **60**, 1081 (1988); J. Phys. A **21**, L517 (1988); **22**, 951 (1989).
[21]M. Holzer, Phys. Rev. B **38**, 1709 (1988); **38**, 5756 (1988); **44**, 2085 (1991).
[22]J. Q. You, J. R. Yan, and Q. B. Yang, Z. Phys. B **80**, 119 (1990).
[23]M. Kolář and M. K. Ali, Phys. Rev. A **39**, 6538 (1989); Phys. Rev. B **39**, 426 (1989); **41**, 7108 (1990).
[24]M. Inoue, T. Takemori, and H. Miyazaki, Solid State Commun. **77**, 751 (1991).
[25]M. Severin, M. Dulea, and R. Riklund, J. Phys. Condens. Matter. **1**, 8851 (1989).
[26]G. Y. Oh, C. S. Ryu, and M. H. Lee, J. Phys. Condens. Matter **4**, 8187 (1992); Phys. Rev. B **47**, 6122 (1993).
[27]J. X. Zhong, T. Xie, J. Q. You, and J. R. Yan, Z. Phys. B **87**, 223 (1992).
[28]M. Severin and R. Riklund, J. Phys. Condens. Matter **1**, 5607 (1989).
[29]G. Y. Oh, C. S. Ryu, and M. H. Lee, J. Korean Phys. Soc. (to be published).
[30]A. Chakrabarti and S. N. Karmakar, Phys. Rev. B **44**, 896 (1991).
[31]J. X. Zhong, J. R. Yan, and J. Q. You, J. Phys. A **24**, L649 (1991).
[32]W. Xu, Solid State Commun. **82**, 645 (1992); J. Q. You, Q. B. Yang, and J. R. Yan, Phys. Rev. B **41**, 7491 (1990).
[33]M. Kolář, M. K. Ali, and I. I. Satija, Phys. Rev. B **40**, 11 083 (1989); J. Q. You, J. R. Yan, and J. X. Zhong, J. Math. Phys. **33**, 3901 (1992).
[34]M. Ishida, H. Kato, N. Sano, and H. Terauchi, J. Phys. Soc. Jpn. **61**, 3428 (1992).
[35]M. Dulea, M. Johansson, and R. Riklund, Phys. Rev. B **42**, 3680 (1990).
[36]C. Godrèche and J. M. Luck, Phys. Rev. B **45**, 176 (1992).
[37]V. Kumar and G. Ananthakrishna, Phys. Rev. Lett. **59**, 1476 (1987); V. Kumar, J. Phys. Condens. Matter **2**, 1349 (1990).
[38]H. Böttger and G. Kasner, Phys. Status Solidi B **162**, 489 (1990).
[39]C. S. Ryu, G. Y. Oh, and M. H. Lee (unpublished).
[40]D. H. Dunlap, H. L. Wu, and P. W. Phillips, Phys. Rev. Lett. **65**, 88 (1990).